Doubly Thermosensitive Self-Assembly of Diblock Copolymers in Ionic Liquids

Takeshi Ueki,[†] Masayoshi Watanabe,*,[§] and Timothy P. Lodge*,[†,‡]

Departments of Chemistry and Chemical Engineering & Materials Science, University of Minnesota, 207 Pleasant Street SE, Minneapolis, Minnesota 55455, and Department of Chemistry & Biotechnology, Yokohama National University, 79-5 Tokiwadai, Hodogaya-ku, Yokohama 240-8501, Japan

ABSTRACT: We describe the doubly thermosensitive micellization-unimer-inverse micellization self-assembly of diblock copolymers in ionic liquids (ILs). Well-defined diblock copolymers (PBnMA(11)-*b*-PNIPAm and PBnMA(22)-*b*-P(NIPAm-*r*-AAm)) were prepared by reversible addition−fragmentation transfer (RAFT) polymerization, where BnMA, NIPAm, and AAm refer to benzyl methacrylate, *N*-isopropyl acrylamide, and acrylamide, respectively. The typical hydrophobic ILs 1-ethyl-3-methylimidazolium bis(trifluoromethane sulfonyl)imide ($[C_2mim][NTf_2]$), 1-butyl-3-methylimidazolium hexafluorophosphate ($[C_4mim]PF_6$), and a 1:1 mixture were selected as solvents. Both PNIPAm and P(NIPAm-*r*-AAm) exhibit an upper critical solution temperature (UCST) phase diagram in these ILs, whereas PBnMA has a lower critical solution temperature (LCST). Consequently, at low temperature, the copolymers formed micelles with PNIPAm cores, whereas above the LCST of the PBnMA, inverse micelles with PBnMA cores were formed. Single polymer chains (unimers) were observed at intermediate temperatures. This doubly thermosensitive aggregation behavior was monitored by light scattering intensity and via the hydrodynamic radius obtained by dynamic light scattering.

Introduction

Ionic liquids (ILs) have received considerable attention because of their attractive properties such as negligible vapor pressure, nonflammability, high ionic conductivity, and wide electrochemical window. This promising class of fluids has been called 'designer solvents' because of the tunability of solvation properties by choice of chemical structure of the cation and anion.[1] Composites of ILs and polymers have also recently been recognized to afford new challenges and opportunities in polymer materials science.[2,3] In particular, block copolymer self-assembly in ILs offers potential advantages over conventional low-molar-mass surfactants and lipids in their design flexibility for controlling nanostructure and functionality through molecular weight, composition, architecture, and choice of monomer units.[4−7] In a solvent that dissolves one block but not the other, copolymers form micelles that consist of dense insoluble cores surrounded by soluble coronas.[8] In more concentrated polymer/IL mixtures,[9] the self-assembly process can lead to structures with well-defined long-range order or symmetry, such as body-centered spherical micelles, hexagonally packed cylindrical micelles, bicontinuous double gyroid, and lamellae.[10]

We have reported the phase behavior of several polymers in ILs, particularly in 1-ethyl-3-methylimidazolium bis(trifluoromethane sulfonyl)imide ($[C_2mim][NTf_2]$). Poly(benzyl methacrylate) (PBnMA),[11] random copolymers of PBnMA with styrene (P(BnMA-*r*-St)), with methylmethacrylate (P(BnMA-*r*-MMA)), and P(St-*r*-MMA),[11,12] or poly(ethyl glycidyl ether)[13] show lower critical solution temperature (LCST) phase diagrams. Interestingly, poly(*N*-isopropylacrylamide) (PNIPAm), which has a well-known LCST phase diagram in aqueous medium,[14] exhibits the opposite upper critical solution temperature (UCST) phase separation in an IL.[15] Therefore, by combining appropriate LCST and UCST blocks, one can gen-erate a doubly thermosensitive block copolymer, that is, one that undergoes demicellization at an upper critical micelle temperature (UCMT), followed by micellization with the other block in the core upon heating through a lower critical micellization temperature (LCMT).

Such stimuli-responsive polymers in ILs are of fundamental interest as well as of potential importance in many applications. As reported in our previous work, the volume phase transition of nonvolatile, thermally stable, and hydrophobic (water-immiscible) ion gels could enable the development of environmentally stable smart gel materials for a variety of purposes.[11] The LCST liquid−liquid phase separation of a polymer in an IL[13] could be utilized in extraction and separation processes without the need for solvent evaporation. The utility of the UCST phase behavior of PNIPAm in ILs has recently been demonstrated in the fully reversible micellization-transfer-demicellization block copolymer micelle shuttle between water and ILs[16] and in thermoreversible ion gels made from triblock and pentablock copolymers.[17]

It is possible to obtain both micelles and the inverse micellar structure from the same diblock copolymer by choosing appropriate selective solvents. For example, polystyrene-*b*-poly-butadiene (PSt-*b*-PB) diblock copolymers[18] can form micelles with either PSt cores (in *n*-alkanes) or PB cores (in DMF or MEK). Diblock copolymers of PSt and polyisoprene (PSt-*b*-PI) exhibit a similar type of reverse micellization in PSt-selective solvents (diethyl phthalate, dimethyl phthalate) and in PI-selective solvents (tetradecane, squalane).[10c,19] The stimuli-sensitive micellization/inverse-micellization self-assembly of a block copolymer in a single solvent has been reported only for aqueous solutions triggered by either pH or temperature.[20−22] In many cases, it is preferable to apply physical (e.g., thermal, optical, magnetic) rather than chemical stimuli (e.g., pH, ionic strength, chemical substance) to induce aggregation or deaggregation to increase the number of possible switching cycles. Here we present the micellization-unimer-inverse micellization of doubly thermosensitive block copolymers in ILs (Figure 1). The molecular design presented here is based on the LCST of PBnMA and the UCST of PNIPAm in ILs, respectively. The

* Corresponding authors. E-mail: mwatanab@ynu.ac.jp (M.W.); lodge@umn.edu (T.P.L.).
[†] Department of Chemistry, University of Minnesota.
[‡] Department of Chemical Engineering & Materials Science, University of Minnesota.
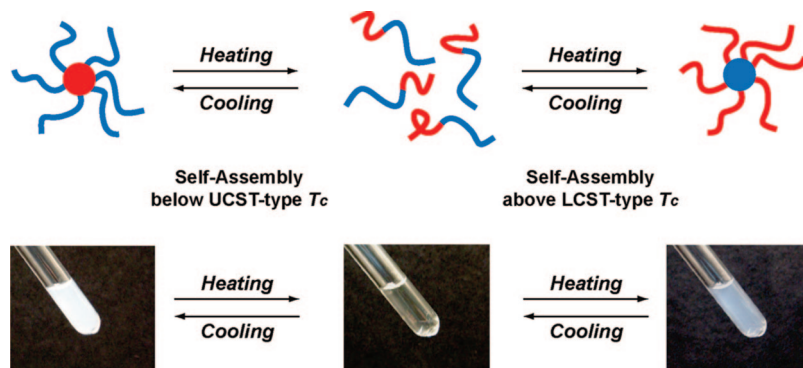[§] Yokohama National University.

Figure 1. Concept of a doubly thermosensitive self-assembly of block copolymers in a single solvent. The red and blue blocks show UCST-type and LCST-type phase behavior, respectively, in the solvent. Photographs show the appearance of a PBnMA(22)-*b*-P(NIPAm-*r*-AAm) 1 wt % [C$_2$mim][NTf$_2$] solution at low, intermediate, and high temperature, respectively.

Scheme 1. Synthetic Procedure for Doubly Thermosensitive Diblock Copolymer PBnMA-*b*-P(NIPAm-*r*-AAm) Using RAFT Polymerization[a]
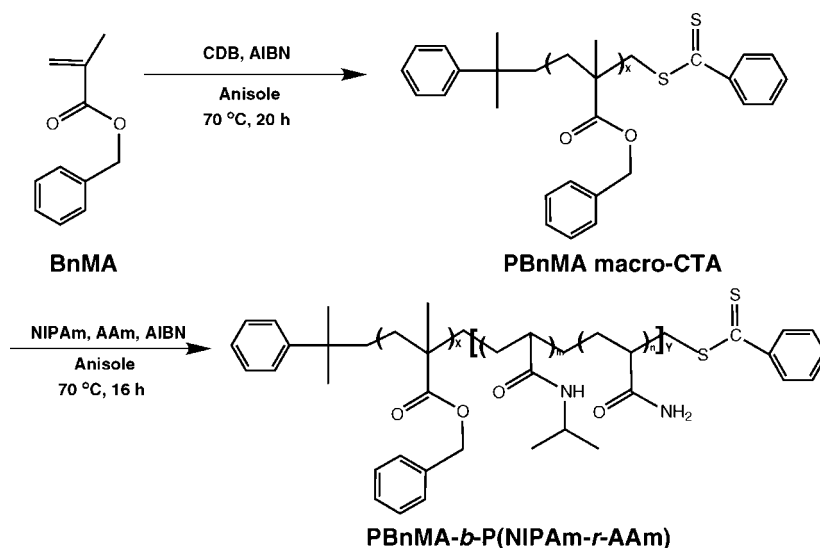
[a] Cumyl dithiobenzoate (CDB) was used as the chain transfer agent (CTA). PBnMA-*b*-PNIPAm was also prepared by a similar protocol.

UCMT and LCMT of both blocks can be manipulated by using IL blends or by decreasing the solubility of a polymer via random copolymerization. Two well-defined block copolymers (PBnMA-*b*-PNIPAm and PBnMA-*b*-P(NIPAm-*r*-AAm)) were prepared by reversible addition−fragmentation chain transfer (RAFT) polymerization,[23] and the micellization properties were studied by light scattering techniques.

Experimental Section

Materials. 1-Butyl-3-methylimidazolium hexafluorophosphate ([C$_4$mim]PF$_6$) was purchased from Solvent Innovation GmbH. 1-ethyl-3-methylimidazolium bis(trifluoromethane sulfonyl)imide ([C$_2$mim][NTf$_2$]) was synthesized and characterized according to a previously reported procedure.[24] All other chemicals were purchased from Aldrich. Benzyl methacrylate (BnMA) monomer was purified by passing through basic alumina columns to remove acidic inhibitor before polymerization. *N*-isopropylacrylamide (NIPAm) was purified by recrystallization (two times) using toluene/hexane (1:10 by weight) mixed solvent. 2,2′-Azobis-isobutyronitrile (AIBN) was recrystallized from methanol prior to use.

Preparation of PBnMA-*b*-PNIPAm and PBnMA-*b*-P(NIPAm-*r*-AAm) Block Copolymers. Doubly thermosensitive block copolymers were prepared by RAFT polymerization.[18,25,26] Here we describe the synthetic procedure for the PBnMA first block, followed by the second block comprising a random copolymer of NIPAm and 3.8 mol % acrylamide (AAm) (Scheme 1). The chain transfer agent (CTA) cumyl dithiobenzoate (CDB) was synthesized and purified by modification of previous methods.[25] BnMA 8.54 g (48.5 mmol), CDB 0.08 g (0.31 mmol), and AIBN 20 mg (0.122 mmol) were dissolved in 20 mL of anisole. The solution was deaerated three times by freeze−pump−thaw degassing, and polymerization was carried out at 70 °C for 20 h. The products were purified by reprecipitation three times from toluene as a good solvent and hexane as a poor solvent. The obtained light-pink powder of PBnMA homopolymer was collected and dried under vacuum and used as a macro-CTA. The structure was confirmed by ^{1}H NMR in CHCl$_3$-*d*$_1$. The conversion was found to be 75%.

Diblock copolymer PBnMA-*b*-P(NIPAm-*r*-AAm) was synthesized using 1 g of the PBnMA macro-CTA (4.54×10^{-5} mol), 0.21 g AAm (2.99 mmol), 6.41 g NIPAm (56 mmol), and 3.1 mg AIBN (1.87×10^{-5} mol) dissolved in 20 mL of anisole. Solutions were degassed by freeze−pump−thaw cycles three times, and polymerization was then carried out at 70 °C for 16 h. Polymer products were obtained by reprecipitation twice from toluene/hexane. The conversion of NIPAm was found to be 72%. ^{1}H NMR for PBnMA-*b*-P(NIPAm-*r*-AAm) (CDCl$_3$, δ): 7.2 (5H, s, H$_{arom}$), 4.9 (2H, s, −CH$_2$−C$_6$H$_5$), 4.0 (2.4H, s, −CH−(CH$_3$)$_2$)). The composition of AAm in the second block was calculated to be 3.8 mol % by elemental analysis for carbon and nitrogen (C: 65.95%, H: 9.04%, O: 15.15%, N: 9.81%). PBnMA-*b*-PNIPAm was also

Table 1. Characterization of PBnMA-CTA and Diblock Copolymers

polymer	M_n (kDa)[a]	N_n[b]	M_w/M_n[c]
PBnMA(11)	11.0	62	1.13
PBnMA(22)	21.8	124	1.14
PBnMA(11)-*b*-PNIPAm	18.9	62−70	1.15
PBnMA(22)-*b*-P(NIPAm-*r*-AAm)	99.3	124−696	1.16

[a] Number-average molecular weight, M_n, of PBnMA-CTA was estimated by GPC. The M_n of block copolymers was calculated from the results of elemental analysis based on the M_n of precursor obtained from GPC. [b] Number-average degree of polymerization. [c] M_w/M_n was determined by GPC in tetrahydrofuran (THF) with 1 vol % tetramethylethylenediamine (TMEDA).

prepared and characterized in the same manner, except there was no AAm in the second step.

Number-average molecular weights (M_n) of the block polymers were calculated by elemental analysis (nitrogen) combined with size exclusion chromatography (SEC) analysis of the PBnMA macro-CTA. PDIs were determined by SEC. The SEC system consists of three Phenogel (Phenomenex) columns with pore sizes of 10^3, 10^4, and 10^5 Å. The eluent was tetrahydrofuran (THF) containing 1 vol % tetramethylethylenediamine (TMEDA). The characterization results of all polymers are shown in Table 1. All four prepared polymers exhibited narrow polydispersity (<1.2). SEC profiles of block copolymers were also unimodal without the high-molecular-weight species indicative of uncontrolled polymerization. In the RAFT polymerization process, polymerization kinetics can be significantly changed because of differences in the chemical structures of monomers.[27] For PBnMA(22)-*b*-P(NIPAm-*r*-AAm) polymerization, to maintain monomer composition of the second block close to the initial feed, NIPAm was randomly copolymerized with the chemically similar AAm, which allowed us to decrease the solubility of the block (leading to an increase in the UCST-type phase separation temperature in an IL).

Dynamic Light Scattering Measurements. All DLS samples were prepared by the cosolvent evaporation method. Block copolymer was first dissolved in THF. Then, an appropriate amount of IL ([C$_2$mim][NTf$_2$] or 1:1 by weight mixture of [C$_2$mim][NTf$_2$] and [C$_4$mim]PF$_6$) was added to the homogeneous THF solution. The solution was then filtered with 0.45 μm PTFE syringe filters to remove dust. The volatile THF was evaporated by heating at 75 °C with stirring under reduced pressure for at least 12 h. After the addition of each solution to a DLS tube (i.d. 0.51 cm), the tube was flame-sealed to prevent any contamination. Polymer solutions were investigated using a home-built photometer equipped with a Brookhaven BI-DS photomultiplier, and a Lexel Ar$^+$ laser operating at 488 nm. DLS measurements were made with the assistance of a Brookhaven BI-9000 correlator. Temperatures were controlled to within ± 0.2 °C using an index-matching silicon oil bath. Experiments were performed at various temperatures from 5 to 200 °C, and the intensity correlation functions $g_2(q,t)$ were recorded at scattering angles between 60 and 120° at each temperature. Samples were equilibrated for 20 min before data collection.

For solutions containing monodisperse particles, the electric field correlation function $g_1(q,t)$ displays a single exponential decay

$$g_1(q, t) = \exp(-\Gamma t) = \exp(-D_0 q^2 t) \tag{1}$$

where q is the scattering vector ($q = (4\pi n/\lambda) \sin(\theta/2)$, where n is the refractive index of the solution, λ is the wavelength of the light in vacuum, and θ is the scattering angle), Γ is the decay rate, and D_0 is the mutual diffusion coefficient at infinite dilute limit. The recorded $g_2(q,t)$ is related to $g_1(q,t)$ through the Siegert relation.[28] The hydrodynamic radius, R_h, can be estimated with knowledge of the solvent viscosity, η, by using the Stokes−Einstein equation

$$R_h = (k_B T)/6\pi\eta D_0 \tag{2}$$

For solutions that contain polydisperse particles, $g_1(q,t)$ can be analyzed using the method of cumulants[29]

$$g_1(q, t) = A \exp(-\Gamma t)(1 + (1/2!)\mu_2 t^2 + ...) \tag{3}$$

where Γ is the mean decay rate, and μ_2/Γ^2 characterizes the width of the distribution. In this work, the apparent hydrodynamic radius, R_h, was calculated using eq 2 by substituting $D = \Gamma/q^2$ of 1 wt % solutions for D_0. The distribution of R_h was also examined by applying the inverse Laplace transformation to $g_1(q,t)$ through the well-established CONTIN program[30] and, in one case, by a sum of two exponentials.

To estimate R_h, the temperature dependence of the viscosity of [C$_2$mim][NTf$_2$] and [C$_4$mim]PF$_6$ was calculated from the appropriate Vogel−Tammann−Fulcher (VTF) equations.[24,31] The temperature dependence of the viscosity of [C$_2$mim][NTf$_2$]/[C$_4$mim]PF$_6$ was also calculated from the VTF equation with consideration of the molar ratio between two ILs. The refractive indices of the ILs were obtained from previous reports.[7,12]

Results and Discussion

PBnMA(11)-*b*-PNIPAm. Figure 2a shows the temperature dependence of the scattering intensity of 1 wt % PBnMA(11)-*b*-PNIPAm in the [C$_2$mim][NTf$_2$]/[C$_4$mim]PF$_6$ mixed solvent (1:1 by weight). The scattering intensity measured at each temperature at an angle of 90° was divided by that measured at 50 °C. This result clearly indicates that the diblock copolymer micellizes below ∼30 °C, near the UCST of PNIPAm, and also above 130 °C, the LCST of PBnMA. The UCST of PNIPAm in [C$_4$mim]PF$_6$ is higher than that in [C$_2$mim][NTf$_2$],[16] and thus the UCMT can be tuned by mixing the two ILs.[32] The molecular origin of the higher UCST in [C$_4$mim]PF$_6$ is not yet clear; however, it is generally accepted that the solvation power and polarity of an IL strongly depends on the chemical structure of the anion.[24,31b,33] We previously reported that whereas the solubility of PNIPAm in molecular solvents could not be correlated with the magnitude of the Lewis acidity (acceptor number; AN), it could be correlated with the Lewis basicity (donor number; DN). In low DN solvents such as chlorobenzene, nitrobenzene, nitromethane, 1,2-dichloroethane, and propylene carbonate, PNIPAm was not soluble at low temperatures; however, it became soluble with increasing temperature.[15] It is conceivable that [C$_4$mim]PF$_6$, having a lower DN than [C$_2$mim][NTf$_2$], makes the solubility of PNIPAm worse, resulting in a higher UCST.

The temperature dependence of the hydrodynamic radius, R_h, for PBnMA(11)-*b*-PNIPAm in [C$_2$mim][NTf$_2$]/[C$_4$mim]PF$_6$ IL blend is shown in Figure 2b. The dual temperature sensitivity and the UCMT and LCMT are both clearly evident. The size of the micelle with a PBnMA core and a PNIPAm corona at high temperature is larger than that of the micelle at low temperature, even though the molecular weights of each block are similar. This suggests that the structures of the two micelles are different. We speculate that the glassy micellar core at low temperature provides one possible explanation of the smaller size than that observed at high temperature. The glass-transition temperatures, T_g, of bulk PNIPAm, bulk PBnMA, [C$_2$mim]-[NTf$_2$], and [C$_4$mim]PF$_6$ are 135, 54, −87, and −77 °C, respectively. From the Gordon−Taylor equation, the T_g of the PNIPAm core would be near 25 °C only when the core is swollen by more than 32 wt % of the IL [C$_2$mim][NTf$_2$]/[C$_4$mim]PF$_6$ blend. (The T_g of [C$_2$mim][NTf$_2$]/[C$_4$mim]PF$_6$ mixed solvent is −82 °C from the Gordon−Taylor equation.) Because this would be a substantial amount of solvent, it is reasonable to infer that the cores are in fact glassy, thereby inhibiting equilibration of micelle structure. It is also possible that there is some preferential partitioning of [C$_2$mim][NTf$_2$] in the core given that the UCST of this solvent is much lower. In such a case, the interfacial tension between swollen core and solvent would be less, favoring the formation of smaller micelles. In contrast, the self-assembly of the block copolymer
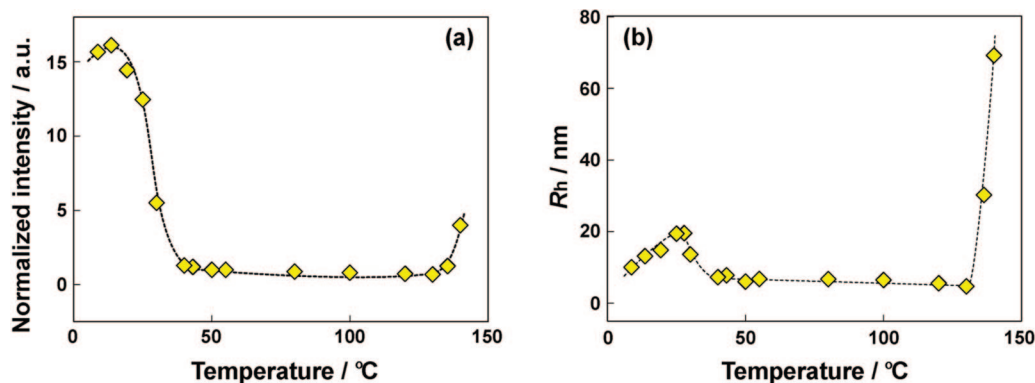
Figure 2. (a) Normalized scattering intensity for PBnMA(11)-*b*-PNIPAm in an IL mixture at a scattering angle of 90°. Normalized intensity is defined as the intensity at each temperature divided by that measured at 50 °C. (b) Temperature dependence of the hydrodynamic radius (obtained by cumulant analysis) of PBnMA(11)-*b*-PNIPAm in the IL blend, which contains 1:1 [C$_2$mim][NTf$_2$]/[C$_4$mim]PF$_6$ (by weight).
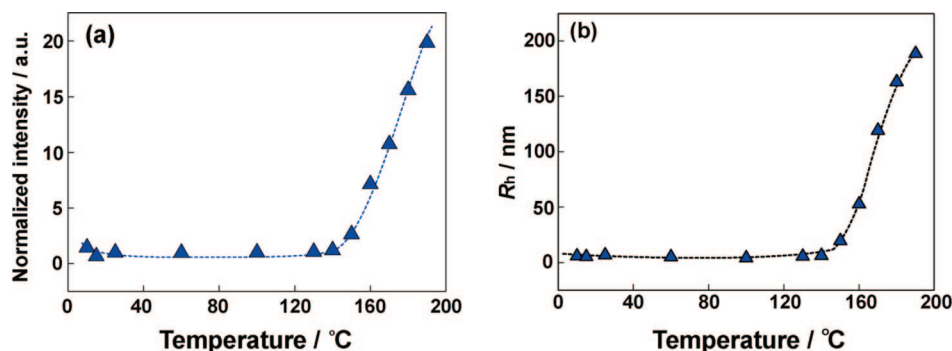

Figure 3. Temperature dependence for PBnMA(11)-*b*-PNIPAm in [C$_2$mim][NTf$_2$] 1 wt % solution: (a) normalized scattering intensity and (b) R_h from cumulant analysis.

at high temperatures features a rubbery core micelle. There is also a hint in Figure 2b of the low-temperature micelles contracting upon further cooling, which could reflect a contraction of the corona blocks.

To explore the high temperature micelle structure in more detail, we extended measurements to higher temperature. However, after heating above 180 °C, there was evidence of polymer degradation. This presumably reflects the fact that the PF$_6$ anion can generate acidic products such as HF,[34] which could induce decomposition of the polymer. When the sample was kept below 140 °C, no noticeable decomposition was observed. Therefore, to access higher temperatures above the LCMT, pure [C$_2$mim][NTf$_2$] was used as the solvent.

Figure 3a shows the temperature dependence of the normalized scattering intensity for PBnMA(11)-*b*-PNIPAm 1 wt % in pure [C$_2$mim][NTf$_2$], and Figure 3b shows the corresponding R_h. A significant increase in scattering intensity and R_h above 140 °C are observed, but in this case, there is no evidence of micellization at low temperature. This presumably results from the lower UCST of PNIPAm in this solvent. In our previous study, the UCST in 1 wt % [C$_2$mim][NTf$_2$] solution of PNIPAm homopolymer with M_n = 15.4 kDa (M_w/M_n = 1.64) was approximately 20 °C.[15] The M_n and the concentration of PNIPAm segment shown in Figure 3 are similar, but the covalently connected, well-solvated PBnMA block suppresses the critical micelle temperature below 5 °C, the lower limit of the current apparatus. Similar results have been reported in other systems, namely, that micellization occurs at a lower temperature than phase separation of the corresponding block.[19]

PBnMA(22)-*b*-P(NIPAm-*r*-AAm). To observe the doubly thermosensitive aggregation using pure [C$_2$mim][NTf$_2$], we prepared a diblock copolymer PBnMA(22)-*b*-P(NIPAm-*r*-AAm). PAAm also shows UCST phase behavior in [C$_2$mim]-

[NTf$_2$], but at much higher temperatures than PNIPAm; for example, the cloud point of 3 wt % PAAm (M_n = 100 kDa, M_w/M_n = 2.2) in [C$_2$mim][NTf$_2$] solution lies above 150 °C. Therefore, random copolymerization of NIPAm with a small amount of AAm can decrease the compatibility of the second block with the IL. We also increased the molecular weight of both blocks, particularly the second one. (See Table 1.) Figure 4a shows the normalized scattering intensity of PBnMA(22)-*b*-P(NIPAm-*r*-AAm) in [C$_2$mim][NTf$_2$] 1 wt % solution, and Figure 4b shows the corresponding R_h. These results confirm that PBnMA(22)-*b*-P(NIPAm-*r*-AAm) exhibits the full sequence of a UCMT, unimers at intermediate temperature, and high-temperature inverse micelles above the LCMT. The micelles at low temperature were significantly larger than before, which is consistent with the increased molecular weight of the P(NIPAm-*r*-AAm) block. Furthermore, the system was fully reversible, even after heating up to 190 °C.

To investigate the distribution of micelle sizes, Laplace inversion of the correlation functions was performed. The CONTIN results at representative low, intermediate, and high temperatures are shown in Figure 5. The narrow, intense peaks above 100 nm clearly indicate the formation of well-defined micelles at both low and high temperatures (Figure 5a,c). However, a broad peak around 200 nm can still be seen in the CONTIN results at 100 °C, where most of the block copolymers are unimers (Figure 5b). The total intensity obtained here is relatively weak compared with the peaks shown in Figure 5a,c. (See Figure 4a.) The R_h from the smaller peak (peak top; 12.7 nm) corresponds to single polymer chains. The larger one indicates that a few P(NIPAm-*r*-AAm)-core micelles remain even at this temperature, a phenomenon that was not seen for PBnMA(11)-*b*-PNIPAm. We speculate that this arises from the composition distribution of AAm in the second block. Although
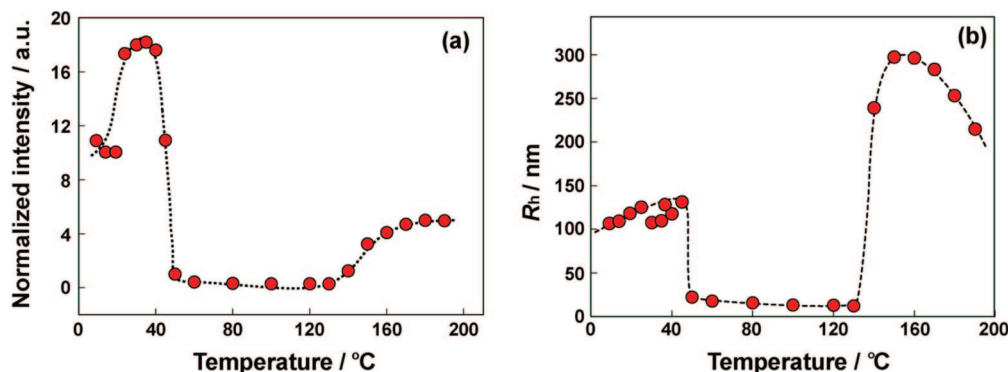
Figure 4. Temperature dependence for PBnMA(22)-*b*-P(NIPAm-*r*-AAm) in [C$_2$mim][NTf$_2$] 1 wt % solution: (a) normalized scattering intensity and (b) R_h from cumulant analysis (except for the intermediate temperature range, as discussed in the text).
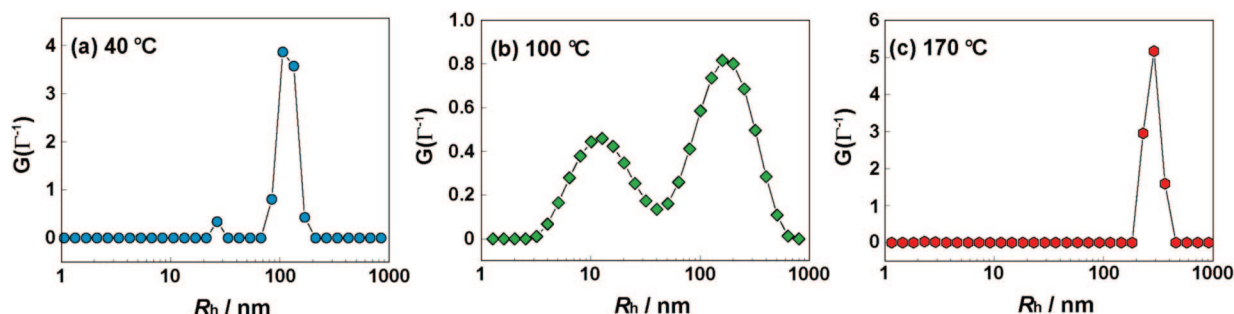

Figure 5. CONTIN results for PBnMA(22)-*b*-P(NIPAm-*r*-AAm) in [C$_2$mim][NTf$_2$] (1 wt %) solution at: (a) 40 °C (low-temperature region; core: PNIPAm-*r*-AAm, shell: PBnMA); (b) 100 °C (intermediate temperature region; single polymer chains with small number of aggregates); and (c) 170 °C (high-temperature region; core: PBnMA, shell: PNIPAm-*r*-AAm).

the average composition of AAm was determined to be 3.8 mol % from elemental analysis, the random copolymer will possess a certain comonomer distribution from chain to chain. Chains with the highest AAm content will be much more insoluble in this solvent, leading to a few persistent micelles. However, as the analysis below reveals, the number of these micelles is small.

Recently, Shibayama and coworkers proposed an analysis of bimodal (or multimodal) dynamic light scattering (DLS) correlation functions to evaluate the weight fraction, $w(R_h)$, of a small amount of large aggregates in a dilute solution.[35] In the case where $qR_1 \leq 1.78 < qR_2$, the weight fraction of the smaller component can be described by the following relationship

$$w_1 = [G(\Gamma_1)/R_1^3]/[(G(\Gamma_1)/R_1^3) + (G(\Gamma_2)R_2q^4/1.78^4)] \quad (4)$$

where w and R are the weight fraction and the hydrodynamic radius of the particle, respectively, and $G(\Gamma)$ is the distribution of the decay rate, Γ. Subscripts 1 and 2 refer to the small and large component in solution, respectively. We applied eq 4 to estimate the fraction of single polymer chain and large aggregates from our CONTIN data. The weight fractions of single polymer chains and large aggregates were estimated to be 87.6 and 12.4 wt %, respectively. This result suggests that almost all of the polymer aggregates break down to form single polymer chains. Assuming a typical aggregation number above 100, the number fraction of unimers in this solution is therefore estimated to be >0.999. In Figure 4b, R_h was determined from cumulant analysis at low and high temperature. In the intermediate temperature range (50−130 °C), only R_h for the smaller size particle, calculated from a double exponential fit, was plotted as a function of temperature. The R_h values of large-size aggregates were not included in the plot because they represent such a small number fraction.

It is interesting to note that in this diblock copolymer solution the UCMT increased to around 50 °C because of the lower miscibility of the longer and AAm-copolymerized NIPAm block. However, the LCMT aggregation of PBnMA was not affected by increasing the molecular weight from 11 to 22 kDa. It has been reported that the LCST of PNIPAm in aqueous solution is affected little by the concentration and molecular weight of the polymer,[36] whereas the LCST of aqueous PEO solutions[37] depends on the concentration and molecular weight of polymer. In the case of PBnMA in ILs, the tendency of molecular weight dependence of phase separation temperature is similar to PNIPAm in water.[38] We previously noted that the effect of decreasing the mixing entropy of PBnMA in ILs that underlies the LCST-type phase separation came from the liquid clathrate structure formation of cations around the benzyl group.[2,11,12,39] The cation−π interaction[40] is analogous to hydrophobic hydration of water around the isopropyl side chain of PNIPAm. The absence of a dependence on PBnMA molecular weight of the LCMT observed in this study may also suggest that the solvation of PBnMA by ILs is a similar situation to PNIPAm in aqueous solution.

Conclusions

In this Article, we prepared well-defined diblock copolymers (PBnMA(11)-*b*-PNIPAm and PBnMA(22)-*b*-P(NIPAm-*r*-AAm)) by RAFT-polymerization. The two blocks exhibit opposite thermosensitivity, that is, LCST- and UCST-type phase separation in ILs, respectively. The temperature dependence of R_h of PBnMA(11)-*b*-PNIPAm in an IL blend solution clearly confirmed that thermal stimuli triggered aggregation at both low and high temperature but with a regime of unimers at intermediate temperature. To realize doubly thermosensitive behavior without any decomposition in [C$_2$mim][NTf$_2$], the UCMT of PNIPAm segment could be manipulated by copolymerization with AAm. These results demonstrate that the temperature at which self-assembly of block copolymers in IL occurs can be controlled by the structural design of the polymer as well as that of the solvent. Multi-stimuli-responsive self-assembly of

block copolymers in ILs provides a possible route to various smart materials.

Supporting Information Available: SEC traces of PB-nMA(11), PBnMA(11)-*b*-PNIPAm, PBnMA(22), and PBnMA(22)-*b*-P(NIPAm-*r*-AAm). This material is available free of charge via the Internet at http://pubs.acs.org.

References and Notes

(1) (a) Welton, T. *Chem. Rev.* **1999**, *99*, 2071. (b) Wasserscheid, P.; Keim, W. *Angew. Chem., Int. Ed.* **2000**, *39*, 3772. (c) Plechkova, N. V.; Seddon, K. R. *Chem. Soc. Rev.* **2008**, *37*, 123. (d) Part A: Properties and Structure. In *Ionic Liquids III: Fundamentals, Progress, Challenges, and Opportunities*; Rogers, R. D., Seddon, K. R., Eds.; ACS Symposium Series 901; American Chemical Society: Washington DC, 2005. (e) Part B: Transformations and Processes. In *Ionic Liquids III: Fundamentals, Progress, Challenges, and Opportunities*; Rogers, R. D., Seddon, K. R., Eds.; ACS Symposium Series 901; American Chemical Society: Washington DC, 2005.

(2) Ueki, T.; Watanabe, M. *Macromolecules* **2008**, *41*, 3739.

(3) Lodge, T. P. *Science* **2008**, *321*, 50.

(4) *Amphiphilic Block Copolymers: Self-Assembly and Applications*; Alexandridis, P., Lindman, B., Eds.; Elsevier: Amsterdam, 2000.

(5) Hawker, C. J.; Wooley, K. L. *Science* **2005**, *309*, 1200.

(6) Lodge, T. P.; Bang, J. A.; Li, Z. B.; Hillmyer, M. A.; Talmon, Y. *Faraday Discuss.* **2005**, *128*, 1.

(7) (a) Li, Z. B.; Kesselman, E.; Talmon, Y.; Hillmyer, M. A.; Lodge, T. P. *Science* **2004**, *306*, 98. (b) Zhou, Z. L.; Li, Z. B.; Ren, Y.; Hillmyer, M. A.; Lodge, T. P. *J. Am. Chem. Soc.* **2003**, *125*, 10182.

(8) (a) He, Y.; Li, Z.; Simone, P.; Lodge, T. P. *J. Am. Chem. Soc.* **2006**, *128*, 2745. (b) Simone, P.; Lodge, T. P. *Macromol. Chem. Phys.* **2007**, *208*, 339.

(9) Simone, P. M.; Lodge, T. P. *Macromolecules* **2008**, *41*, 1753.

(10) (a) Bates, F. *Science* **2003**, *251*, 898. (b) Lodge, T. P.; Pudil, B.; Hanley, K. J. *Macromolecules* **2002**, *35*, 4707. (c) Hanley, K. J.; Lodge, T. P. *Macromolecules* **2000**, *33*, 5918.

(11) Ueki, T.; Watanabe, M. *Langmuir* **2007**, *23*, 988.

(12) Ueki, T.; Karino, T.; Kobayashi, Y.; Shibayama, M.; Watanabe, M. *J. Phys. Chem. B* **2007**, *111*, 4750.

(13) Tsuda, R.; Kodama, K.; Ueki, T.; Kokubo, H.; Imabayashi, S.; Watanabe, M. *Chem Commun.* **2008**, 4939.

(14) Schild, H. G. *Prog. Polym. Sci.* **1992**, *17*, 163.

(15) Ueki, T.; Watanabe, M. *Chem. Lett.* **2006**, *35*, 964.

(16) Bai, Z.; He, Y.; Young, N. P.; Lodge, T. P. *Macromolecules* **2008**, *41*, 6615.

(17) (a) He, Y.; Lodge, T. P. *Chem. Commun.* **2007**, 2732. (b) He, Y.; Lodge, T. P. *Macromolecules* **2008**, *41*, 167.

(18) Oranli, L.; Bahadue, P.; Riess, G. *Can. J. Chem.* **1985**, *63*, 2691.

(19) Lodge, T. P.; Bang, J.; Hanley, K. J.; Krocak, J.; Dahlquist, S.; Sujan, B.; Ott, J. *Langmuir* **2003**, *19*, 2103.

(20) Dimitrov, I.; Trzebicka, B.; Müller, A. H. E.; Dworak, A.; Tsvetanov, C. B. *Prog. Polym. Sci.* **2007**, *32*, 1275.

(21) (a) Bütün, B.; Armes, S. P.; Billingham, N. C.; Tuzar, Z.; Rankin, A.; Eastoe, J.; Heenan, R. K. *Macromolecules* **2001**, *34*, 1503. (b) Cai, Y.; Armes, S. P. *Macromolecules* **2004**, *37*, 7116. (c) Wang, D.; Yin, J.; Zhu, Z.; Ge, Z.; Liu, H.; Armes, S. P.; Liu, S. *Macromolecules* **2006**, *39*, 7378.

(22) (a) Arotçaréna, M.; Heise, B.; Ishaya, S.; Laschewsky, A. *J. Am. Chem. Soc.* **2002**, *124*, 3787. (b) Weaver, J. V. M.; Armes, S. P.; Bütün, V. *Chem. Commun* **2002**, 2122. (c) Maeda, Y.; Mochiduki, H.; Ikeda, I. *Macromol. Rapid Commun.* **2004**, *25*, 1330.

(23) (a) Mayadunne, R. T. A.; Rizzardo, E.; Chiefari, J.; Chong, Y. K.; Moad, G.; Thang, S. H. *Macromolecules* **2000**, *33*, 243. (b) Moad, G.; Rizzardo, E.; Thang, S. H. *Aust. J. Chem.* **2005**, *58*, 379. (c) Moad, G.; Chiefari, J.; Krstina, J.; Postma, A.; Mayadunne, R. T. A.; Rizzardo, E.; Thang, S. H. *Polym. Int.* **2000**, *49*, 993.

(24) Tokuda, H.; Hayamizu, K.; Ishii, K.; Susan, M. A. B. H.; Watanabe, M. *J. Phys. Chem. B* **2005**, *109*, 6103.

(25) Perrier, S.; Barner-Kowollik, C.; Quinn, J. F.; Vana, P.; Davis, T. P. *Macromolecules* **2002**, *35*, 8300.

(26) Nakayama, M.; Okano, T. *Biomacromolecules* **2005**, *6*, 2320.

(27) (a) Chong, B. Y. K.; Krstina, J.; Le, T. P. T.; Moad, G.; Postma, A.; Rizzardo, E.; Thang, S. H. *Macromolecules* **2003**, *36*, 2256. (b) Chiefari, J.; Mayadunne, R. T. A.; Moad, C. L.; Moad, G.; Rizzardo, E.; Postma, A.; Skidmore, M. A.; Thang, S. H. *Macromolecules* **2003**, *36*, 2273.

(28) *Dynamic Light Scattering: The Method and Some Applications*; Brown, W., Ed.; Clarendon Press: Oxford, England, 1993.

(29) Koppel, D. E. *J. Chem. Phys.* **1972**, *57*, 4814.

(30) Provencher, S. W. *Comput. Phys. Commun.* **1982**, *27*, 213.

(31) (a) Tokuda, H.; Hayamizu, K.; Ishii, K.; Susan, M. A. B. H.; Watanabe, M. *J. Phys. Chem. B* **2004**, *108*, 16593. (b) Tokuda, H.; Tsuzuki, S.; Susan, M. A. B. H.; Hayamizu, K.; Watanabe, M. *J. Phys. Chem. B* **2006**, *110*, 19593.

(32) Bai, Z.; He, Y.; Lodge, T. P. University of Minnesota, Minneapolis, MN, unpublished results.

(33) (a) Swiderski, K.; McLean, A.; Gordon, C. M.; Vaughan, D. H. *Chem. Commun.* **2004**, 2178. (b) Lee, S. H.; Lee, B. B. *Chem. Commun.* **2005**, 3469. (c) Santos, L. M. N. B. F.; Canongia, L. J. N.; Coutinho, J. A. P.; Esperanca, J. M. S. S.; Gomes, L. R.; Marrucho, I. M.; Rebelo, L. P. N. *J. Am. Chem. Soc.* **2007**, *129*, 284.

(34) (a) Najdanovic-Visak, V.; Esperanca, J. M. S. S.; Rebelo, L. P. N.; Ponte, M. N.; Guedes, H. J. R.; Seddon, K. R.; Szydłowski, J. *Phys. Chem. Chem. Phys.* **2002**, *4*, 1701. (b) Swatloski, R. P.; Holbrey, J. D.; Rogers, R. D. *Green Chem.* **2003**, *4*, 361.

(35) Shibayama, M.; Karino, T.; Okabe, S. *Polymer* **2006**, *47*, 6446.

(36) Azevedo, R. G.; Rebelo, L. P. N.; Ramos, A. M.; Szydłowski, J.; Sousa, H. C.; Klein, J. *Fluid Phase Equilib.* **2001**, *185*, 189.

(37) (a) Saeki, S.; Kuwahara, N.; Nakata, M.; Kaneko, M. *Polymer* **1976**, *17*, 685. (b) Bae, Y. C.; Lambert, S. M.; Soane, D. S.; Prausnitz, J. M. *Macromolecules* **1991**, *24*, 4403.

(38) Okada, Y.; Tanaka, F. *Macromolecules* **2005**, *38*, 4465.

(39) (a) Holbrey, J. D.; Reichert, W. M.; Nieuwenhuyzen, M.; Sheppard, O.; Hardacre, C.; Rogers, R. D. *Chem. Commun.* **2003**, 476. (b) Deetlefs, M.; Hardacre, C.; Nieuwenhuyzen, M.; Sheppard, O.; Soper, A. K. *J. Phys. Chem. B* **2005**, *109*, 1593. (c) Łachwa, J.; Szydłowski, J.; N-Visak, V.; Rebelo, L. P. N.; Seddon, K. R.; Ponte, M. N.; Esperança, J. M. S. S.; Guedes, H. J. R. *J. Am. Chem. Soc.* **2005**, *127*, 6542. (d) Łachwa, J.; Bento, I.; Duarte, M. T.; Lopes, J. N. C.; Rebelo, L. P. N. *Chem. Commun.* **2006**, 2445. (e) Łachwa, J.; Szydłowski, J.; Makowska, A.; Seddon, K. R.; Esperança, J. M. S. S.; Guedes, H. J. R.; Rebelo, L. P. N. *Green Chem.* **2006**, *8*, 262.

(40) Ma, J. C.; Dougherty, D. A. *Chem. Rev.* **1997**, *97*, 1303.